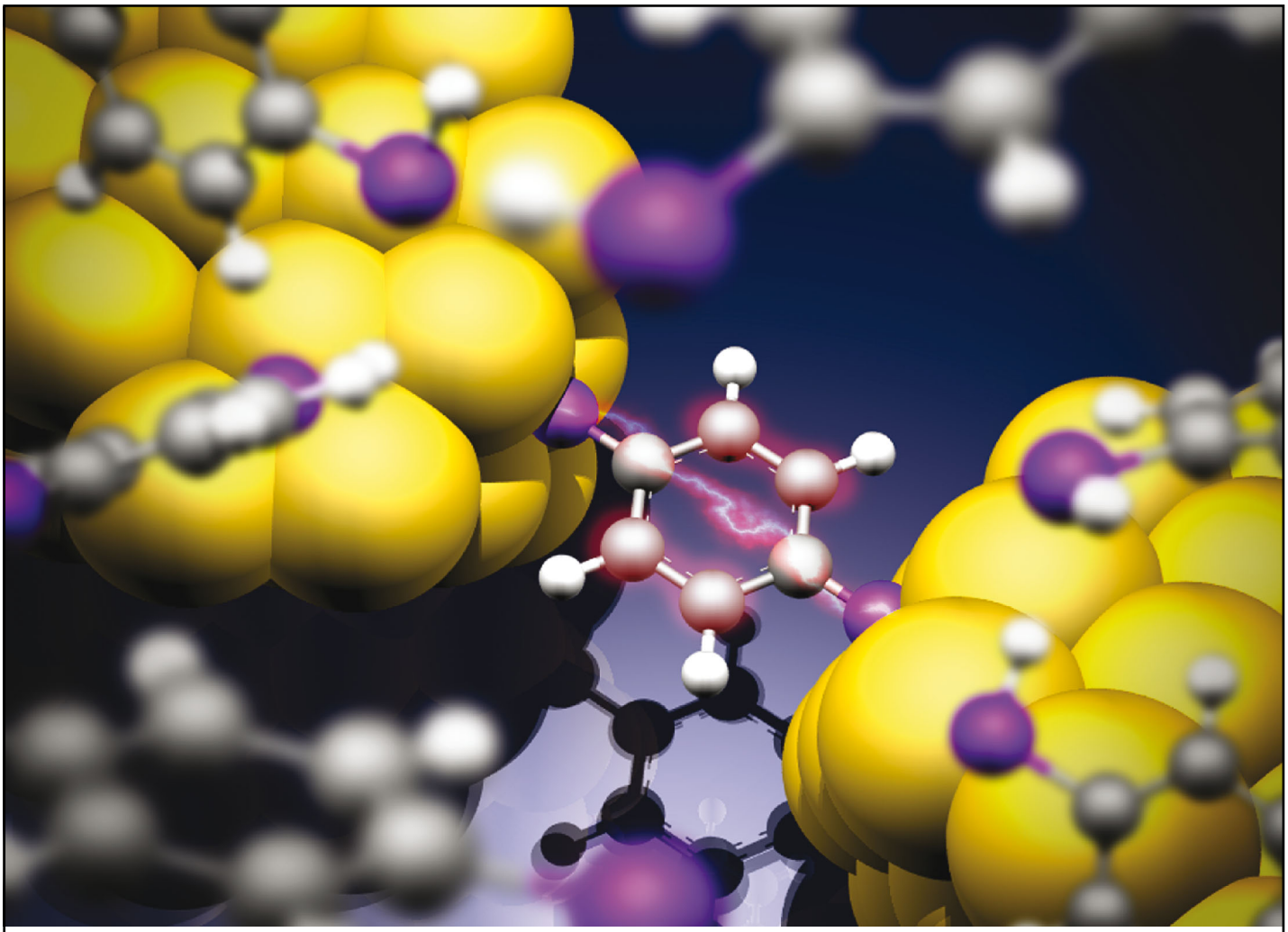

**Showcasing research from the Molecular Structure Laboratory, Tokyo Institute of Technology, Japan.**

**Title: Single molecule bridging between metal electrodes**

The paper presents a single molecule junction where a single molecule bridges between metal electrodes. A single molecule junction is a low-dimensional material having two metal–molecule interfaces. Due to its geometrical and electronic characters, single molecular junctions show novel properties that are not observed in isolated molecular or bulk systems.

**As featured in:**


See Kiguchi and Kaneko, *Phys. Chem. Chem. Phys.*, 2013, **15**, 2253.

**www.rsc.org/pccp**

Registered Charity Number 207890

PCCP

RSC Publishing

PERSPECTIVE

View Article Online
View Journal | View Issue



# Single molecule bridging between metal electrodes

Manabu Kiguchi* and Satoshi Kaneko

Cite this: *Phys. Chem. Chem. Phys.*, 2013, **15**, 2253

Received 7th November 2012,
Accepted 27th November 2012

DOI: 10.1039/c2cp43960c

**www.rsc.org/pccp**

Single molecular junctions, in which a single molecule bridges between metal electrodes, have attracted wide attention as novel properties can appear due to their peculiar geometrical and electronic characters. The single molecular junction has also attracted attention due to its potential application in ultrasmall single molecular electronic devices, where single molecules are utilized as active electronic components. Thus, fabrication of single molecular junctions as well as understanding and controlling their properties (*e.g.* conductance, optical and magnetic properties) have become long-standing goals of scientists and engineers. This review article focuses on the experimental aspects of single molecular junctions, with primary focus on the electron transport mechanism.

## Introduction

A single molecular junction, where a single molecule bridges between metal electrodes, is a low-dimensional material having two metal–molecule interfaces (Fig. 1). Due to their geometrical and electronic characters, single molecular junctions can show novel properties that are not observed in isolated molecular or bulk systems. The single molecular junction has also attracted attention due to its potential application in ultrasmall electronic devices.[1–9] The utilization of single molecules as active components in electronic devices leads to a drastic decrease in device size, and increases in the density of the devices and the calculation speed. The utilization of a single molecule in electronic devices has another advantage. The recent development of synthetic techniques makes it possible to design the properties of molecules. The performance of devices can thus be freely controlled by choosing the appropriate molecule and designing its properties. Molecules are mainly made of carbon (C), hydrogen (H), nitrogen (N), and oxygen (O), all of which are present in large amounts on Earth. Hence, high-performance electronic devices can be fabricated without using rare earth elements.

The utilization of single molecules in electronic devices was first proposed by Aviram and Ratner in 1974.[10] They theoretically predicted the diode properties of a molecular junction where a donor π system and an acceptor π system were connected with an insulating part (methylene). In 1997, Reed *et al.* succeeded in fabricating a single molecular junction of

*Department of Chemistry, Graduate School of Science and Engineering, Tokyo Institute of Technology, 2-12-1 W4-10 Ookayama, Meguro-ku, Tokyo 152-8551, Japan. E-mail: kiguti@chem.titech.ac.jp; Fax: +81-3-5734-2071; Tel: +81-3-5734-2071*

**Manabu Kiguchi**

*Manabu Kiguchi received his PhD in surface science in* 2000 *from Tokyo University. In* 1999, *he joined Prof. Koichi Saiki's group as an assistant professor in Tokyo University and worked on insulating thin films. In* 2004, *he joined Prof. Kei Murakoshi's group as a lecture in Hokkaido University, where he studied single molecule junctions. In* 2005, *he joined Prof. Jan van Ruitenbeek's group in Leiden University. In* 2009, *he was appointed to the position of associate professor at Tokyo Institute of Technology. His current research interests are focused on the nanomaterials including single molecule junction.*

**Satoshi Kaneko**

*Satoshi Kaneko has studied the electrical properties of single molecular junctions since he joined Prof. Kiguchi's group in* 2009. *He received BS degree in* 2010 *and MS degree in* 2012 *from Tokyo Institute of Technology. He has been a PhD candidate at Tokyo Institute of Technology and JSPS Research Fellow since April* 2012.

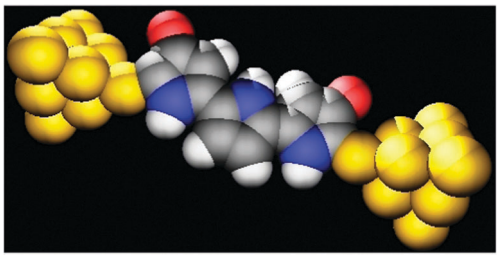

**Fig. 1** Schematic view of a single molecular junction, in which a single molecule bridges between metal electrodes.

1,4-benzenedithiol (BDT) using the mechanically controllable break junction (MCBJ) technique at room temperature.[11] In 2001, Cui *et al.* measured the conductance of a single octanedithiol molecule using conductive AFM.[12] In 2003, Xu and Tao developed the conventional technique for investigating a single molecular junction using a scanning tunneling microscope (STM).[13] Currently, various single molecular junctions have been fabricated and their electron transport properties have been investigated.[14–17] Properties of single molecular junctions can be controlled by external stimuli such as gate voltage, light, electrochemical potential, and force.[18–20] Characterization of the atomic and electronic structures of the single molecular junction is also an important topic in the research field of single molecular junctions. Various techniques (*e.g.*, inelastic electron tunneling spectroscopy (IETS), shot noise, surface enhanced Raman scattering (SERS)) have been applied to single molecular junctions in order to characterize them further.[21–23]

The electric current through the single molecular junction is represented by the Landauer-Büttiker formula:

$$I(V) = \frac{2e}{h}\int_{-\infty}^{\infty} \mathrm{d}E\tau(E)[f_{\mathrm{L}}(E) - f_{\mathrm{R}}(E)] \qquad (1)$$

where $f_{\mathrm{L}}(E)$, $f_{\mathrm{R}}(E)$, $\tau(E)$, $e$, and $h$ are the Fermi distribution functions of the left and right electrodes, the transmission of the single molecular junction, elementary electric charge, and Planck's constant, respectively. The electron transport mechanism depends on many factors, such as the strength of the metal–molecule coupling, energy alignment of the single molecular junction, and molecular length. When the energy difference between the conduction orbital and the Fermi level of the metal electrodes is large, electrons transport *via* a simple tunneling mechanism, where conductance exponentially decreases with the length of the molecule. When the energy difference between the conduction orbital and the Fermi level of the metal electrodes is not as large and the strength of the coupling between molecule and metal electrodes is not as small, electrons transport *via* a resonant tunneling mechanism. Assuming that one molecular level (HOMO or LUMO) dominates transport, as is often the case in molecular junctions, the transmission function is represented by Lorentzian:

$$\tau(E) = \frac{4\Gamma_{\mathrm{R}}\Gamma_{\mathrm{L}}}{(E-\varepsilon)^2 + (\Gamma_{\mathrm{L}} + \Gamma_{\mathrm{R}})^2} \qquad (2)$$

where $\varepsilon$, $\Gamma_{\mathrm{L}}$ and $\Gamma_{\mathrm{R}}$ are the energy of the conduction orbital, and the coupling between molecule and left and right electrodes, respectively. Under the symmetric coupling condition, zero bias conductance of the single molecular junction can be represented by

$$G = \frac{2e^2}{h}\frac{4\Gamma^2}{\Delta^2 + 4\Gamma^2} \qquad (3)$$

where $\Gamma$ and $\Delta$ are the coupling between the molecule and electrode, and the energy difference between the conduction orbital and the Fermi level of the metal electrode, respectively.[1,3] When the molecular size is large and π-conjugation is broken in the molecule, electrons transport *via* a hopping mechanism.

The conductance of a single molecular junction depends on the intensity of $\Gamma$, $\Delta$, degree of π-conjugation, and other factors, as discussed above. Highly conductive single molecular junctions can be obtained by satisfying the following conditions: strong metal–molecule coupling (large $\Gamma$), small energy difference between the conduction orbital and the Fermi level (small $\Delta$), and a high degree of π-conjugation. Although the resonant tunneling model cannot predict the conductance value accurately, we can roughly understand the electron transport properties of the single molecular junction. In this review, we thus focus on the current topics of single molecular junctions considering the strength of the metal–molecule coupling, energy alignment, and the degree of π-conjugation.

## Fabrication of single molecular junction

Molecular junctions have been fabricated using various techniques, such as nanofabricated gaps, nanoholes, mercury droplets, crossed wires, metal nanoparticles, STM, and conducting tip atomic force microscopy (CAFM). Electron transport properties of small ensembles of molecules have been investigated for the molecular junctions.[1,3,4,24–26] Choi *et al.* succeeded in observing the change in direct-current transport from tunneling to hopping, by investigating the conductance of the conjugated oligophenyleneimine using CAFM.[26] Single molecular junctions can be fabricated using the break junction technique, CAFM, metal nanoparticle dimers, and other techniques.[1,12,27]

In the break junction technique, single molecular junctions are fabricated by breaking metal contacts in the presence of target molecules. The formation process of a single molecular junction is shown in Fig. 2. After breaking the metal contact, several molecules bridge between metal electrodes. The number of molecules bridging the metal electrodes decreases one by one during the stretching process. Finally, a single molecular junction is formed just before breakdown of the junction.

STM break junction (STM-BJ) and MCBJ techniques are the most popular techniques for investigating the single molecular junction. In the STM-BJ technique, the STM tip is repeatedly moved in and out of contact with a substrate.[13,28] Fig. 3 shows the example of conductance change in Au contacts broken in the 0.1 M $NaClO_4$ solutions containing benzenedithiol (BDT).[29] The conductance decreased in a stepwise fashion with each step occurring at an integer multiple of $1.1 \times 10^{-2}$ $G_0$ ($2e^2/h$). The last plateau before the contact break showed a value of $1.1 \times 10^{-2}$ $G_0$. The corresponding histogram showed a feature

 

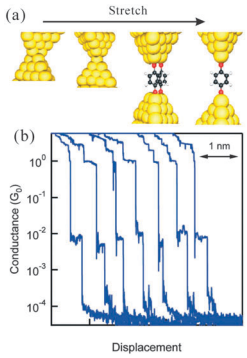


**Fig. 2** (a) Schematic view of the formation process using the break-junction technique. (b) Conductance of the contact during breaking of the Au contact in the presence of the 2-methoxy-1,4-diaminobenzene.[28]

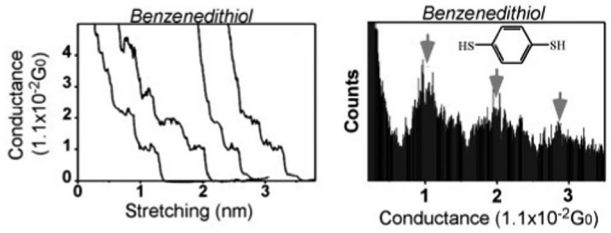


**Fig. 3** (a) Typical conductance traces and (b) conductance histograms of benzenedithiol molecule junctions in 0.1 M $NaClO_4$ solutions.[29]

at $1.1 \times 10^{-2}$ $G_0$. In the absence of BDT, neither plateaus nor peaks were observed in either the conductance traces or histograms below 1 $G_0$. These results indicate that the plateau in the traces and the distinctive features in the conductance histograms, both of which occur at $1 \times 1.1 \times 10^{-2}$ $G_0$ and $2 \times 1.1 \times 10^{-2}$ $G_0$, could be ascribed to bridging of one and of two BDT molecules between the Au electrodes, respectively.

Using STM, Haiss *et al.* developed *I*(s) and *I*(t) methods.[30–32] In the *I*(s) method, the STM tip is first set close to the Au surface. At a certain distance, the stable molecular junctions are formed between the tip and the sample. Next, the tip is lifted while keeping a constant $x$–$y$ position, and the current–relative tip–sample distance relation is measured. In the *I*(t) method, the Au STM tip is held at a given distance above the substrate whilst monitoring current jumps as molecular wires bridging the tip and substrate form and subsequently break. Both the *I*(s) and the *I*(t) method result in the same single-molecule conductance for alkanedithiols.[31]

Fig. 4(a) shows schematic views of MCBJ.[33,34] Notched metal wire is fixed on the elastic substrate, which is covered with an insulator. The substrate is mounted in a three-point bending configuration. The metal wire is mechanically broken by bending the substrate. The bending can be relaxed to form atomic-size contacts between the wire ends using a piezo element for fine adjustment. Single molecular junctions fabricated using MCBJ are more stable than those fabricated using STM-BJ. The stability of the single molecular junction depends on the length of the free standing part ($u$), which can be decreased to submicrometer lengths

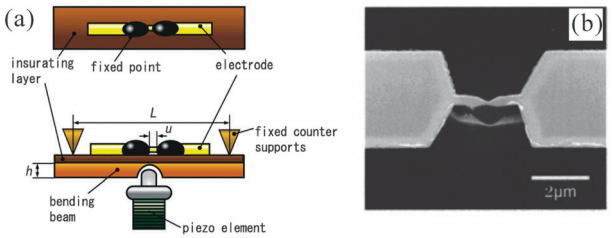


**Fig. 4** (a) Schematic view of MCBJ. (b) SEM image of nano-fabricated Au MCBJ electrodes.[34]

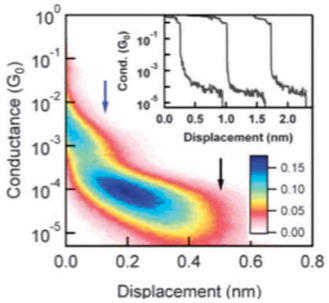


**Fig. 5** 2D conductance histogram for oligosilanes.[36]

using lithographic techniques. Fig. 4(b) shows the SEM image of nano-fabricated Au MCBJ electrodes. Using nano-fabricated MCBJ electrodes, the single molecular junctions can be sustained more than 24 hours.[35] The atomic and electronic structures, as well as the optical, mechanical, and magnetic properties of the single molecular junction have been investigated, thanks to the high stability of single molecular junctions fabricated with MCBJ.[18,22,34]

The formation process of the molecular junction can be investigated by analyzing the conductance traces with the break junction technique. Fig. 5 shows the 2D conductance histogram for oligosilanes. Thousands of traces were used to generate two-dimensional (2D) conductance–displacement histograms.[36] Here, the displacement was defined as the distance relative to the break of the $G_0$ contact. We see an intense peak around $10^{-4}$ $G_0$ that extends for a distance of *ca.* 0.5 nm, indicating that single molecule junctions are formed reproducibly with this molecule and can be elongated over that distance.

## Metal–molecule contact in single molecular junction

In a conventional single molecular junction, molecules are attached to the metal electrodes *via* anchoring groups. The thiol group is the most popular anchoring group and Au is most widely utilized as metal electrodes for single molecular junctions.[1,3–9] This is because stable single molecular junctions can be prepared using a strong covalent Au–S bond. In addition, the chemistry of self-assembled monolayers (SAM) has been investigated in detail. However, the use of a thiol anchoring group poses some inherent disadvantages: first, thiol groups act as resistive spacers between the electrodes and the molecule,

leading to low conductivity of the single molecular junction. Second, the conductance of thiol-based molecular junctions is distributed over a wide range of values, which are ascribed to various metal–molecule configurations. Based on these backgrounds, the development of ideal metal–molecule contact is one of the important topics, since the metal–molecule contact plays the decisive role in determining the mechanical stability and conductance of the single molecular junction. The metal–molecule contact should satisfy the following conditions: (i) forming sufficiently strong bonds between a molecule and metal surfaces (large $\Gamma$), (ii) existence of conducting molecular orbitals close to the Fermi levels to pass electrons or holes through the molecule (small $\Delta$), and (iii) small spread in the conductance values of the conductance of the molecular junction.

Currently, various anchoring groups have been investigated to create mechanically stable and conductive molecular junctions, such as amine ($-NH_2$), isocyanide (–NC), cyanide (–CN), carboxylic acid (–COOH), selenol (–Se), dimethyl phosphine ($-PMe_2$), methyl sulfide (–SMe), pyridine, and $C_{60}$.[37–51] Chen *et al.* investigated the effect of the anchoring group on the conductance of the single molecular junctions of disubstituted alkanes terminated with –SH, $-NH_2$, and –COOH. Fig. 6 shows the conductance of a single disubstituted alkane terminated with –SH, $-NH_2$, and –COOH as a function of molecular length.[38] The conductance decreases with the molecular length, since electrons transport through the molecule *via* a tunneling mechanism. The conductance of the single disubstituted alkane molecular junction decreases in the following order: –SH > $-NH_2$ > –COOH. The order of the conductance of the single molecular junctions is in accordance with the order of the bond strength (Au–S > Au–$NH_2$ > Au–COOH). In the case of the disubstituted alkane molecule, both HOMO and LUMO are far from the Fermi level, and thus, the energy difference between the conduction orbital and the Fermi level ($\Delta$) does not significantly change with the anchoring group. On the other hand, the strength of the metal–molecule coupling ($\Gamma$) changes with the choice of the anchoring group. Therefore, the conductance of the single molecular junction reflects the strength of the metal–molecule coupling. Hong *et al.* investigated the conductance of the single molecular junction using tolane molecules, which have pyridyl (PY), SH, $NH_2$, and CN anchoring groups.[39] The conductance decreased in the following order: –SH > $-NH_2$ > –PY > –CN, Here, again, the order of conductance could be explained by the strength of metal–molecule coupling ($\Gamma$).

The small spread in the conductance values of the molecular junctions is important in the investigation of single molecular junctions and the fabrication of single molecular devices.[40–44] Fig. 7 shows the conductance histograms measured with 1,4-benzenediamine (BDA), 1,4-BDT and 1,4-benzenediisonitrile.[40] The full width at half-maximum of peak in the conductance histogram is much smaller for the BDA than the BDT. The bonding between Au and $NH_2$ is a simple delocalization of the lone pair of electrons from the amine nitrogen to Au atoms. Thus, the Au–$NH_2$ bond is not strongly directional and is relatively insensitive to the local structure, leading to the small spread in the conductance values. A theoretical calculation study has given another reason for the small spread in the conductance values. The strength of the Au–$NH_2$ bond is weak compared to the Au–S bond. The most energetically stable adsorption geometry is possible for the single molecular junction with the Au–$NH_2$ bond, whereas different adsorption geometries with very distinct transport properties can be probable for other anchoring groups (*e.g.* –SH, –NC).[48] Dimethyl phosphines ($-PMe_2$), methyl sulfides (–SMe), and diphenylphosphine ($-PPh_2$) were also found to be promising anchoring groups for obtaining single molecular junctions with well-defined conductance values.[43,44] These anchoring groups have lone pairs, which form non-directional σ bonds with the Au electrodes, leading to small spread in the conductance values of single molecular junction. Mishchenko *et al.* showed that the spread in the conductance values of the single molecular junction with an Au–CN bond was small by investigating single molecular junctions of biphenyl derivatives. The small spread in the conductance values was attributed to the high selectivity of the N–Au binding.[41] Recently, benzene and $C_{60}$ have been used as anchoring units, which weakly interact with the metal electrodes (see Fig. 8).[50,51] The molecules having a $C_{60}$ anchoring unit show small spread in the conductance values, compared to a thiol anchoring unit.

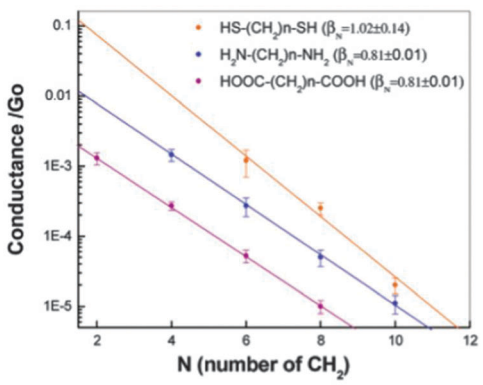


**Fig. 6** Logarithmic plots of single-molecule conductance *vs.* molecular length for dithiol- (orange), diamine- (blue), and dicarboxylic-acid-terminated (purple) alkanes.[38]

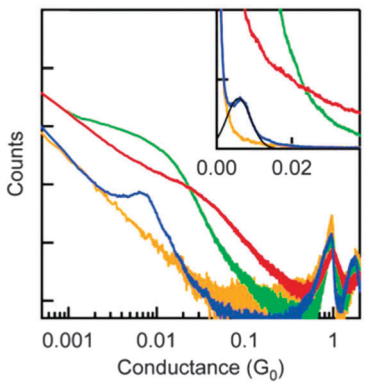


**Fig. 7** Conductance histograms measured in the presence of 1,4-benzenediamine (blue), 1,4-benzenedithiol (red), and 1,4-benzenediisonitrile (green) shown on a log–log plot. The control histogram of Au without molecules is also shown (yellow).[40]

 

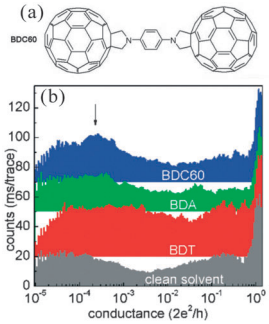


**Fig. 8** (a) Molecular structures of 1,4-bis(fullero[*c*]pyrrolidin-1-yl)benzene(BDC60), (b) conductance histograms of BDC60 and other reference molecules.[51]

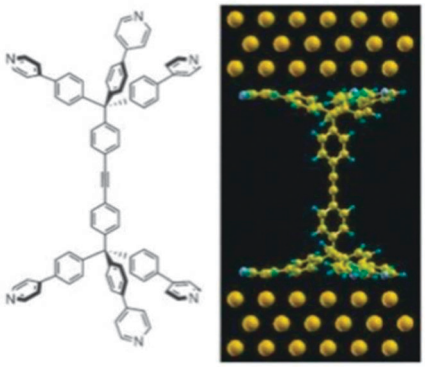

**Fig. 9** Chemical structure of molecules having pyridine-based tripodal anchoring units, together with the optimized structure of junctions.[54]

In order to improve the strength of the metal–molecule coupling ($\Gamma$), utilization of a transition metal is a reasonable strategy. Kiguchi *et al.* succeeded in improving the conductance of the single BDT molecular junction up to 0.03 $G_0$ by using Pt electrodes.[52] This value is the highest conductance value for the single molecular junction with anchoring groups. In the case of Pt, a narrow 5d band is located at the Fermi level, and local density of states is high. Therefore, the metal–molecule coupling is strong for the single molecular junction with the Pt electrode, compared to the Au electrode. Higher conductivity of the single molecular junction with group 10 metals (Pt, Pd) has also been reported for alkanedithiol and alkanediisothiocyanates.[53] Smenario *et al.* calculated the conductance of the single BDT molecular junction for various metal–molecule contacts, and found that Pd is the most promising metal electrode in the case of single BDT molecular junctions.[47] The energy of the molecular orbital varies with the molecules, and it is changed by the interaction between the metal and the molecule. Therefore, the energy difference between the conduction orbital and the Fermi level ($\Delta$) depends on the combination of metal species of the electrodes and the molecule. The conductance of a single molecular junction depends on both the strength of metal–molecule coupling ($\Gamma$) and the energy difference ($\Delta$). Highly conductive single molecular junctions can be obtained by choosing the best metal electrodes for individual molecules bridging between metal electrodes.

The stability and conductance of the single molecular junction can be improved by using multi anchoring units. Ie *et al.* have recently reported a pyridine-based tripodal anchoring unit (see Fig. 9).[54] Due to the tripodal structure, robustness of the surface attachment and control of the molecular orientation were achieved. A pyridine terminal formed electronic π contact by tripodal structures, and high conductance was realized. The multi-anchoring units have been applied to single porphyrin and triangle molecules[55,56] Li *et al.* investigated the single molecular junction of porphyrin with four identical pyridyl substituents using the STM-BJ technique. The molecule binds to the metal electrode *via* two parts instead of four, although the molecule has four anchoring parts. Interestingly, electrons transport through the farthest anchoring groups (*para*-configuration), which contradicts the traditional assumption, *i.e.*; electrons transport *via* the shortest path (*ortho*-configuration).

The anchoring position also affects the conductance of the single molecular junction.[57] Tagami *et al.* performed density functional theory (DFT) calculations for phenalenyl-based molecules connected to semi-infinitely long Au.[58] Their results showed that the doped phenalenyl-based molecule can be transformed from a semiconductive to a metallic conductor by changing the sites connected to electrodes. Similar theoretical approaches have been used to examine the single benzene and porphyrin molecules attached to the electrodes with possible anchoring positions.[59] By applying simple analytical models and/or the Huckel model, the possibility of controlling quantum interference for electron pathways was discussed. In the case of BDT, the conductance of 1,3-BDT was calculated to be smaller than that of the 1,4-BDT.[60] Kiguchi *el al.* have investigated the effect of anchoring positions on conductance of a single molecular junction of BDT and BDA using the STM-BJ technique.[61] Fig. 10 shows the conductance histograms measured with 1,2-, 1,3- and 1,4-BDA. A single molecular junction was not formed for 1,2-BDA, while single molecular junctions were formed for 1,3- and 1,4-BDA. 1,2-BDA molecules adsorb on one of the Au electrodes and would not bind the other side of the Au electrodes (see Fig. 10b). The conductance of the single 1,4-BDA molecular junction was larger than that of the 1,3-BDA. The theoretical calculations satisfactorily reproduced the relationship between the molecular conductance and the anchoring position. The change of the anchoring position from 1,4 to 1,3 in benzene provides deformation of the HOMO as well as its energy-shift,

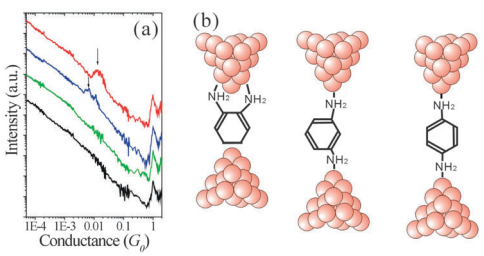


**Fig. 10** (a) Conductance histograms measured in solution without molecules (black) and with 1,2-BDA (green), 1,3-BDA (blue), and 1,4-BDA (red) shown on a log–log plot. (b) Schematic view of the single molecular junction fabricated with the STM break junction technique.[61]

which leads to the change in the conductance of the single molecular junction. On the other hand, electron pathway analysis did not show quantum interference. While interference effect has not been observed for small molecules such as BDA and BDT, clear interference effects have been recently reported for rigid π-conjugated molecular wires containing an anthraquinone unit.[62]

## Direct binding of π-conjugated molecule to metal electrode

In the above discussion, we describe the single molecular junction using anchoring groups. While stable single molecular junctions can be prepared using anchoring groups, the conductance of a single molecular junction is still much lower than that of a metal atomic contact (below 0.03 $G_0$). This is because the anchoring groups act as resistive spacers. To overcome this issue, direct binding of π-conjugated molecules to metal electrodes was recently proposed.[17,63–65] The direct binding technique was first applied to benzene.[17] The single benzene molecular junction was fabricated using MCBJ in ultra-high vacuum at 4.2 K. The single benzene molecular junction was characterized by IETS, shot noise (see Characterization section), and theoretical calculation. The conductance of the single benzene molecular junction is 1 $G_0$ ~ 0.2 $G_0$, depending on the atomic configuration of the single molecular junction. The conductance value is close to that of the metal atomic contact. A highly conductive single molecular junction can be prepared by direct binding of the π conjugated molecule to the metal electrodes. Fig. 11 shows the theoretical calculation result of conductance of the single benzene molecular junction as a function of stretching the junction. The benzene molecule is initially positioned on the Pt electrodes with its plane perpendicular to the Pt junction axis. By stretching the junction, the benzene molecule is progressively tilted with respect to the Pt junction axis, and the conductance and the number of C atoms bonded to the Pt tip atoms decrease. The strength of the molecule–metal coupling ($\Gamma$) decreases *via* tilting, and thus, the conductance of the single benzene molecular junction decreases with stretching.

While the single benzene–Pt molecular junction shows a high conductance value, it does not show a fixed conductance

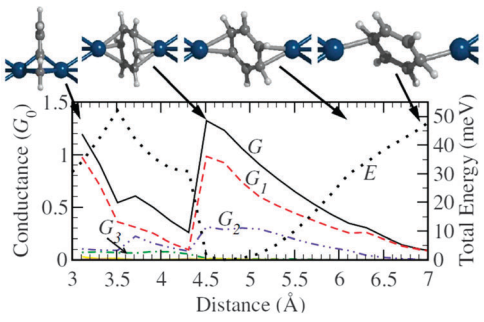


**Fig. 11** Simulation of the stretching process of a Pt–benzene junction: total conductance, $G$; the contribution of the individual transmission channels, $G_i$; and the change of the total energy, $E$, as a function of the distance between the Pt tip atoms.[17]

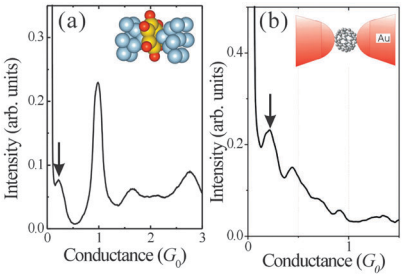


**Fig. 12** (a) Conductance histograms for Ag–benzene molecular junctions measured at 10 K. (b) Conductance histogram for $C_{60}$–Au molecular junctions measured at 300 K.[63]

value. In order to obtain a single benzene molecular junction showing a fixed conductance value, s-metals such as Au and Ag were investigated.[63] Fig. 12(a) shows the conductance histogram of the Ag contacts after the introduction of benzene. The conductance histograms show a peak at 0.2 $G_0$. The IETS spectrum of the junction showed a peak around 42 meV, corresponding to the vibrational mode between benzene and Ag. The most energetically stable single benzene molecular junction was formed during the stretching of the Ag contact in the presence of benzene. When the single benzene–Ag junction is stretched, the junction breaks due to weak interaction between the benzene molecule and the Ag electrodes. In contrast, the benzene–Pt junction is able to take various atomic configurations during the stretching of the junction due to the strong metal–molecule interaction, which induces featureless conductance histograms. The moderate metal–molecule interaction is favorable for obtaining the single molecular junction showing a fixed conductance value.

The direct binding technique has been applied to other molecules, such as $C_{60}$, endohedral Ce@$C_{82}$ metallofullerenes, ethylene and acetylene.[63–65] These single molecular junctions also show high conductance values. The conductance of the single $C_{60}$–Au, $C_{60}$–Ag and $C_{60}$–Pt molecular junctions are 0.3 $G_0$, 0.5 $G_0$, and 0.7 $G_0$, respectively, as shown in Fig. 12(b).[63] The metal dependence of conductance of the single $C_{60}$ molecular junction is explained by the strength of the metal–molecule coupling ($\Gamma$). The relative bond strength is Pt–$C_{60}$ > Ag–$C_{60}$ > Au–$C_{60}$. The $C_{60}$ molecule adsorbs on the Pt surface *via* a strong covalent bond, while the $C_{60}$ molecule weakly adsorbs on the Au surface without forming a covalent bond. Reflecting the strength of the metal–molecule coupling, conductance of the single $C_{60}$–Pt molecular junction is higher than that of the $C_{60}$–Au and $C_{60}$–Ag molecular junctions. It is noteworthy that the single $C_{60}$–Pt molecular junction shows a fixed conductance value in contrast to the single benzene–Pt junction. During the junction stretching, the out-of-plane molecular orientation does not change due to the spherical molecular shape of $C_{60}$, although the in-plane molecular orientation could change. Therefore, the $C_{60}$ single molecular junction shows a fixed conductance value.

Taniguchi *et al.* applied the direct binding technique to tetrathiafulvalene (TTF) and tetraselenafulvalene (TSF) molecular junctions. These molecules are connected to Au electrodes in a face-to-face configuration. The conductance of the single

 

TTF and TSF molecular junctions are 0.02 $G_0$ and 0.003 $G_0$, respectively, which are low in comparison to other $C_{60}$ and benzene molecular junctions.[66]

The coupling between the π orbital of molecules and metal electrodes was reported for a single pentaphenylene molecular junction. Changing the angle of the molecule from a highly tilted state to an orientation nearly perpendicular to the electrodes changes the conductance by one order of magnitude. The conductance of the single pentaphenylene molecular junction follows $G \sim \sin^4\theta$, where $\theta$ is the tilting angle. This conductance behavior qualitatively agrees with theoretical models of molecular π-orbitals coupling to a metal electrode. The authors proved the bridging of the molecule by observation of the conductance change synchronized with a fast mechanical perturbation in the lateral and horizontal plane.[67] A bipyridine molecule could also bind to the metal electrodes *via* a direct N–Au bond and lateral coupling of π orbitals. Quek *et al.* succeeded in performing mechanically-controlled binary conductance switching of a single bipyridine molecular junction.[68] The high and low conductance states were assigned to the molecular junction, where the bipyridine molecule sat in a tilted and a parallel configuration with respect to the junction axis, respectively. In the tilting configuration, the Au s-state and the LUMO π* orbital couple and thus, the strength of the molecule–metal coupling ($\Gamma$) is enhanced.

The direct Au–C bonding was reported using a trimethyltin ($SnMe_3$) anchoring group. The C–$SnMe_3$ bond was cleaved and the Au–C bond was formed when the Au contacts were broken in the presence of the disubstituted alkane molecule terminated with $SnMe_3$. The conductance of the single alkane molecular junction with the direct Au–C bond was 100 times larger than that with a conventional anchoring group–metal bond (*cf.* Au–S, Au–$NH_2$).[69]

## Electron transport mechanism through single molecular junction

In this section, we discuss the experimental investigation on the basic mechanism of the electron transport through single molecular junctions.

In the tunnelling mechanism,[1,3,4] conductance of the single molecular junction is represented by

$$G = A_N \exp(-BL) \quad (4)$$

The $B$ value depends on the degree of π-conjugation, HOMO–LUMO gap, and the energy difference between the metal electrode and the molecular orbital ($\Delta$). The $B$ values are 2.0 $Å^{-1}$, 0.7 ∼ 0.9 $Å^{-1}$, and 0.05 ∼ 0.2 $Å^{-1}$ for vacuum gap, alkane, and π-conjugated molecules, respectively.[1,3,4] The development of the single molecule wire with a small $B$ value is one of the most current research topics. Sedghi *et al.* succeeded in decreasing the $B$ value to 0.04 $Å^{-1}$ by putting metal ions into an oligoporphyrin molecular wire.[15,70] Here, it is noteworthy that they found that the conductance of the single molecular wire depends on temperature. Although it is widely accepted that such behaviour is a signature of a thermally assisted incoherent (hopping) mechanism,[1,3,4] theoretical calculation results revealed that electrons transport *via* a tunnelling mechanism. The observed temperature dependence is explained by the broadening of the Fermi distribution function. Yamada *et al.* revealed that the electron transport mechanism changed from tunnelling to hopping around 5.6 nm using long oligothiophene molecules.[71]

Venkakaranan *et al.* investigated the relationship between the degree of π conjugation and conductance of the single molecular junction using biphenyl molecules.[14] The twist angle ($\theta$) between two rings is controlled by choosing the substituent groups. The conductance of the single biphenyl molecular junction decreases with $\theta$ ($G \propto \cos^2\theta$). As the twist angle between the two rings increases, the degree of π-conjugation between them decreases, causing a decrease in the conductance of the single molecular junction. A similar relationship between the twist angle ($\theta$) between the two rings and the conductance has been observed for $(NH_3)_5$Ru-4,4′-bipy-Ru$(NH_3)_5$.[72]

The relationship between energy level alignment and conductance has been investigated using substituted BDA.[28] Fig. 13 shows the conductance of a single substituted BDA molecular junction as a function of calculated ionization potential for the series of 12 molecules tested. Electron-donating substituents, which drive the HOMO up (small ionization potential), increase the conductance, while electron-withdrawing substituents have the opposite effect. In the single BDA molecular junction, electrons transport through HOMO, and thus, the conductance increases as the energy difference between the HOMO and the Fermi level ($\Delta$) decreases. Dell'Angela *et al.* investigated the relationship between electronic energy level alignment at a metal–molecule interface and single molecular conductance using photoemission spectroscopy.[73] They clearly showed that the energy difference between the HOMO and the Fermi level for the three molecules adsorbed on Au(111) correlates well with changes in conductance.

Xu *et al.* succeeded in controlling the difference between the conduction orbital and the Fermi level of metal electrodes ($\Delta$) with electrochemical potential.[74,75] Fig. 14 shows the current through the single phenylthiol-terminated perlene tetracarboxylic diimide molecular junction as a function of the electrochemical potential. The current can be controlled reversibly over two to three orders of magnitude with the electrochemical potential, and reaches a peak near the redox potential of the molecule, where the energy of the molecular orbital agrees with the Fermi level of the metal electrodes ($\Delta = 0$).[74,75] The difference

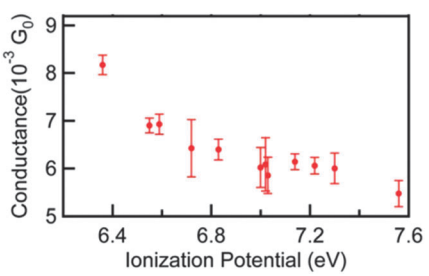


**Fig. 13** Conductance values against the calculated ionization potential of the single substituted BDA molecular junction.[28]

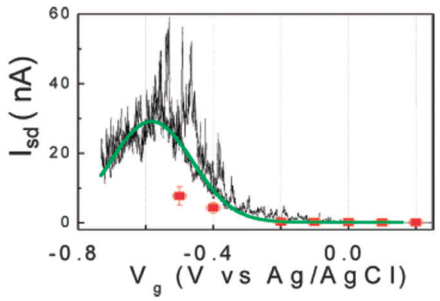


**Fig. 14** Current through the single phenylthiol-terminated perlene tetracarboxylic diimide molecular junction as a function of the electrochemical potential.[75]

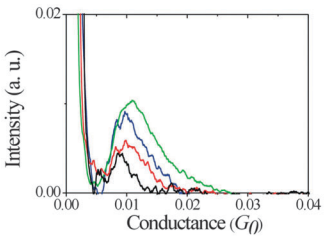


**Fig. 15** Conductance histograms of Au contacts in tetraglyme (green), water (red), and mesitylene (blue) containing 10 mM BDA. The black curve represents the result measured in $N_2$ gas. The tunneling background has been subtracted.[78]

between the conduction orbital and the Fermi level of metal electrodes ($\Delta$) can also be controlled by the electric field in solid state molecular devices.[18] Similar conductance enhancement caused by a decrease in the electrochemical potential was observed for the single molecular junction of 6-[1′-(6-mercapto-hexyl)-[4,4]bipyridinium]-hexane-1-thiol iodide.[30] The conductance enhancement is attributed to the one-electron reduction of the bipyridinium moiety (V) from $V^{2+}$ to the radical $V^{+}$.

## Effect of environment on single molecular junction

The conductance behavior of the single molecular junction is affected by the environment. Tawara *et al.* calculated the spread in conductance values of the single BDT molecular junction in water.[76] They showed that water molecules affected the dynamics, and more specifically, the C–S stretching mode of the single molecular junction. The conductance of the single BDT molecular junction depends on the length of the C–S bond; thus, the spread in the conductance value is suppressed in water compared to that in vacuum. Fatemi *et al.* investigated the conductance of a single BDA molecular junction.[77] The solvent could increase the conductance of a single BDA molecular junction by as much as 50%. The solvent-induced shift in conductance is explained by the shift of the work function of the Au contact induced by the solvent binding to undercoordinated Au sites around the junction. The increase in the Au contact work function reduces the difference between the Au Fermi energy and the conduction orbital ($\Delta$), which leads to the increase in the conductance of the single molecular junction.

Nakashima *et al.* investigated the effect of the environment on spread in the conductance value of the single 1,4-BDA molecular junction.[78] The conductance of the single BDA molecular junction in tetraglyme, mesitylene, water, and $N_2$ gas decreased in that order, while the spread in the conductance value increased (see Fig. 15). The order of the conductance values of the single BDA molecular junction was explained by the strength of the interaction between solvent molecules and Au electrodes. The order of the spread in the conductance values was explained by the diversity in the coverage of the BDA molecule at metal electrodes and atomic and molecular motion of the single molecular junction. The atomic and molecular motion of the junction was suppressed in the order of $N_2$ gas, water, mesitylene, and tetraglyme, reflecting the molecular weight and viscosity of the solvent. When the atomic and molecular motion of the single molecular junction is suppressed, the conductance of the junction does not significantly change with time, leading to a decrease in the spread in the conductance values. The spread in the conductance values can also be explained by the coverage of the BDA molecule. The coverage of BDA molecules on an Au electrode decreased in the order of $N_2$ gas, water, mesitylene, and tetraglyme, reflecting the strength of the interaction between the Au electrode and the solvent. The amount of the charge transfer from the BDA molecule to Au (decrease in conductance value) was largest for the single BDA molecular junction in $N_2$ gas, compared to the single BDA molecule bridging clean Au electrodes. The spread in the conductance values of single molecular junction increased with change in the conductance value compared to the single BDA molecule bridging clean Au electrodes.

The effect of water on conductance of the single molecule junction was investigated using ologothiophene-containing molecular wire.[79] The effect was larger for the longer molecular wire. The conductance can be over 2 orders of magnitude larger in the presence of water. The theoretical calculation supported the obtained experimental results. The enhancement of conductance is attributed to the electron transfer between water and molecules.

## Electron transport through π stack system

Recent development of the experimental technique of the single molecular junction enables us to investigate the basic electron transport mechanism at a single molecular level. Electron transport through the non-covalently bound, π-stacked systems has been of particular interest and plays a vital role in biological systems, organic electronics, and polymer and materials science, typically at the macroscopic level and in bulk.[80] However, electron transport through the π-stacked systems has never been directly examined because creating molecular junctions of stacked π-molecules between electrodes is nontrivial. Recent development of synthetic techniques makes it possible to arrange the π molecules in the controlled manner. Kiguchi *et al.* have succeeded in investigating electron transport through a π-stack system using the π-stack molecules (Fig. 16a).[16] Schneebeli *et al.* also succeeded in investigating electron transport through

 

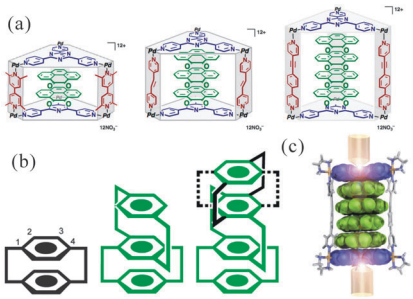


**Fig. 16** (a) Structure of π-stacked molecules, (b) structure of π-stacked benzene rings, (c) schematic view of the single π-stack molecular junction.

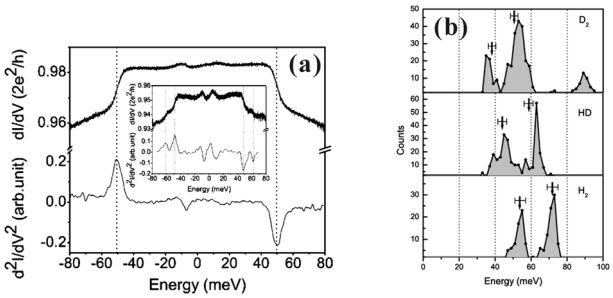


**Fig. 17** (a) Differential conductance (top) and its derivative (bottom) of the single $D_2$–Pt junction. (b) Distribution of vibration energy for $H_2$, HD, $D_2$–Pt junctions.[22]

π-stacked systems using stacked benzene rings held together in an eclipsed fashion *via* a paracyclophane scaffold (Fig. 16b).[81]

The atomic configuration of the single π-stacked systems was characterized by the conductance change during the breaking process of the single molecular junction. The analysis showed that top and bottom triangular aromatic panels of the π-stacked molecules were bound to the Au electrodes, as shown in Fig. 16(c).

In general, the conductance of a short molecular junction is given by eqn (4). The $B$ value for single-molecule π-stacked molecules is 0.1 $Å^{-1}$, derived from the slope of $L$ *vs.* ln $G$ plots, and is smaller than that of insulating alkane chains ($B$ = 0.7 ∼ 0.9 $Å^{-1}$), and comparable to that of conductive π-conjugated organic molecules ($B$ = 0.05 ∼ 0.2 $Å^{-1}$). The small $B$ value for single-molecule π-stacked molecules indicates the efficient electron transport through a π stacked system. In the case of the π-stacked benzene rings, the $B$ value was 0.63 $Å^{-1}$, which was smaller than the value observed for alkanes, but larger than that of the π-stacked molecules.[81]

The electron transport through the π-stacked system can be also investigated for molecules attached to one side of the metal electrodes.[82,83] Wu *et al.* investigated the conductance of oligo-phenylene ethynylene (OPE) molecules with two anchoring groups, only one of which was a thiol. Significant electron transport was observed even for the OPE molecules with only one thiol anchoring group. Electrons are transported through the aromatic π–π coupling between adjacent molecules. The electron transport through π-stacked systems has also been investigated using theoretical investigations.[84,85]

## Characterization of single molecular junction

While various single molecular junctions have been investigated, most of these studies only investigated the conductance of the single molecular junction. To fully understand the electron transport properties of the single molecular junction, characterization of the junction is critically important. There are experimental challenges to characterizing the atomic and electronic structures of the single molecular junction. IETS, point contact spectroscopy (PCS), and SERS have been applied to single molecular junctions in order to characterize their atomic configurations; thermo power, shot noise, and transition voltage spectroscopy have been applied in order to characterize their electronic structure.

Vibration spectroscopy of the single molecular junction (IETS, PCS) provides the information on its atomic configuration. The differential conductance is measured as a function of the bias voltage across the junction. The conductance changes above the threshold voltage, which corresponds to the excitation of the vibration mode of the junction; its vibration spectroscopy was applied to the $H_2$ molecule.[22] Currently, this technique has been applied to various single molecular junctions including benzene, water, alkanedithiol, $C_{60}$, ethylene, acetylene.[17,86,87]

Fig. 17(a) shows the example of differential conductance ($dI/dV$) of the single $D_2$–Pt molecular junction as a function of voltage.[22] A symmetric downward step in the differential conductance was observed around 50 mV, and peaks were observed in its derivative ($d^2I/dV^2$). The downward step in $dI/dV$ indicates the excitation of vibrational modes by conduction electrons with energies of 50 meV. In order to determine the vibrational energy accurately, a large number of differential conductance spectra were collected for the $H_2$, HD, $D_2$–Pt junctions. Fig. 17(b) shows the distribution of these vibrational energies. The histogram shows a well-defined peak at 54 meV and 72 meV for $H_2$. These two peaks are expected to shift with the mass $m$ of the isotopes as $\omega^2 \propto 1/m$. This agrees with the observations, as shown by the scaled position of the hydrogen peaks marked by arrows above the distributions for $D_2$ and HD.

Conductance change by excitation of the vibration mode is an interesting issue in the vibration spectroscopy of single molecular junctions. This excitation leads to increases in the junction conductance at the tunneling regime (low conductance regime: IETS), while it leads to decreases in the junction conductance at the contact regime (high conductance regime: PCS). The increase and decrease in conductance are explained by forward scattering and backscattering of electrons that lose energy to a vibration mode. Paulsson *et al.* showed that the conductance change by this vibration mode excitation depends on the conductance of the single molecular junction and symmetry of the coupling of the molecule to metal electrodes. In the case of symmetric coupling, theoretical calculations have predicted the crossover between increase and decrease in the junction conductance at a transition probability of 0.5. The experimental results for $H_2$, $H_2O$ benzenedithiol junctions actually showed that the transition between increases and decreases in junction conductance was around 0.5 $G_0$.[88–90]

SERS is a promising technique for studying the geometrical structure and the dynamical motion of a single molecule

junction. A strong electric field is formed between the nano-gap electrodes, and thus, the Raman spectrum from the molecule in the nano-gap is selectively observed in the case of the single molecular junction. In addition, SERS can be performed even under the condition at room temperature with relatively large thermal fluctuation, while other vibration spectroscopy, such as IETS and PCS, can be measured only at low temperatures in UHV. Due to these advantages of SERS, simultaneous measurements on conductance and SERS of a single molecular junction have been carried out.[23,91,92] Tian *et al.* succeeded in combining the SERS and MCBJ methods, and observed an enhancement of the SERS intensity with decreasing gap size. Ward *et al.* and Konishi *et al.* reported the simultaneous measurements on conductance and SERS of the molecular junction (Fig. 18).[91] They observed the appearance of the b2 modes for the molecular junction, which was not observed for the bulk crystal. Liu *et al.* observed the broadening of Raman peak for the single molecular junction and the peak energy shift induced by the bias voltage using "fishing mode" tip enhanced Raman spectroscopy.[23] The peak energy shift was attributed to the change in the binding energy between the molecule and metal electrodes.

The electronic structure of the single molecule junction can be investigated using transition voltage spectroscopy (TVS). TVS has been applied to conjugated molecular wires by Frisbie *et al.* They observed the minimum in the ln $(I/V^2)$–$1/V$ curve (Fowler–Nordheim plot).[26] The minimum voltage ($V_m$) is assigned to the transition voltage, where the electron transport mechanism changes from the direct tunneling mechanism at low bias voltage to the field emission or F–N tunneling mechanism at high bias voltage. They discussed that $V_m$ scaled linearly with the energy difference between the conduction orbital and the Fermi level of metal electrodes ($\Delta$), referring to the Simmons model for tunneling. The Simmons model

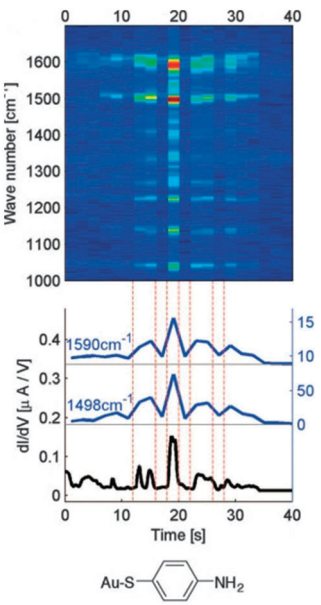


**Fig. 18** Waterfall plot of the Raman spectrum and the positively correlated conductance measurement for a *p*-mercaptoaniline sample.[91]

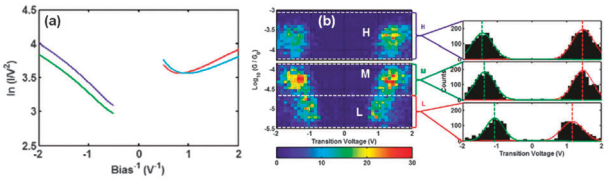


**Fig. 19** (a) Transition voltage spectroscopy for the single alkanedithoil molecular junction. (b) 2-D transition voltage histograms for single alkanedithoil molecular junction at three different conductance regimes (H, M, L).[95]

assumes the tunneling barrier, and the barrier is tilted when a bias voltage is applied. On the other hand, the single molecular junction is not a simple tunneling barrier. There are discussions as to whether the molecule bridging the metal electrodes can be regarded as a tunneling barrier. The F–N plot is also considered based on the resonant tunneling model. Here, the minimum in the ln $(I/V^2)$-$1/V$ curve is ascribed to the voltage, where the molecular level approaches the edge of the bias window.[93,94]

Fig. 19 shows the TVS of the alkanedithoil molecular junctions, showing three different conductance values (H, M and L).[95] L-junctions show smaller transition voltage values than those for H- and M-junctions, which indicates that the difference between the HOMO and the Fermi level of metal electrodes ($\Delta$) for L-junctions is smaller than those of H- and M-junctions, despite their lower conductance values. The L-junction has been attributed to a gauche conformation, and the theoretical calculation supports a smaller HOMO-Fermi gap for the L-junctions. The smaller transition voltage for L-junctions is explained by the smaller energy difference between the conduction orbital and the Fermi level ($\Delta$).

The energy difference between the conduction orbital and the Fermi level ($\Delta$) can be obtained by measuring the thermopower of the single molecular junction. The Seebeck coefficient of the single molecular junction can be represented by

$$S_{\text{Seebeck}} = \frac{-\pi^2 k_B^2 T}{3e} \frac{\partial \ln(T(E))}{\partial E}\bigg|_{E=E_F} \quad (5)$$

where $k_B$, $T$, and $T(E)$ are the Boltzmann constant, temperature, and transmission function, respectively. By comparing the Seebeck coefficient of the single molecular junction and transmission function obtained by the theoretical calculation, the energy level alignment can be evaluated. Reddy *et al.* measured the Seebeck coefficient for a single 1,4-benzenedithiol (BDT) molecular junction. The positive sign unambiguously indicates p-type (hole) conduction in the single molecular junction, that is, HOMO is close to the Fermi level. The Seebeck coefficient measurement and theoretical calculation results revealed that the Au Fermi level position was 1.2 eV above the HOMO level of BDT.[21] It is noteworthy that the conductance is sensitive to the number of molecules bridging the metal electrodes and the strength of the metal–molecule coupling, but the Seebeck coefficient is not sensitive to these values.[96,97]

The breaking process of a single molecular junction was investigated using AFM.[98] Fig. 20 shows the force curve during

 

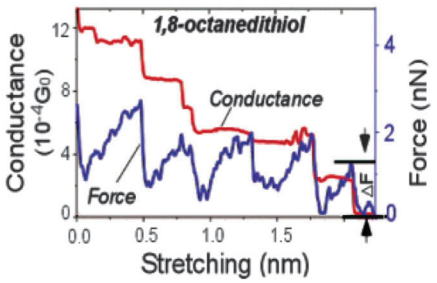


**Fig. 20** Simultaneously recorded conductance and force curves of alkanedithiol molecular junction during stretching of the junction.[98]

breaking of the alkanedithiol molecular junction together with the conductance curve. While the conductance decreases in discrete steps, the corresponding force decreases in saw tooth-waves. The force required to break a single alkanedithiol molecular junction is 1.5 nN, which is similar to the force required to break an Au–Au. The Au–Au bond is responsible for the breakdown of the alkanedithiol molecular junction.[98]

The number of molecules bridging the metal electrodes can be determined by simultaneous conductance and shot noise measurements. The shot noise originates from time-dependent fluctuations in the electrical current caused by the discreteness of the electron charge. When electrons flow across the molecular junction, the noise level is determined by the number of available transmission channels across the junction and their transmission probabilities $\tau_i$. The total noise level of a quantum point contact for temperature $T$ and applied bias voltage $V$ is given

$$S_{\text{noise}} = 2\,eV\coth\left(\frac{eV}{2kT}\right)\frac{2e^2}{h}\sum\tau_i(1-\tau_i) + 4k_{\text{B}}T\frac{2e^2}{h}\sum\tau_i^2 \quad (6)$$

On the other hand, the conductance ($G$) of the molecular junction is given by.

$$G = \frac{2e^2}{h}\sum\tau_i \quad (7)$$

Therefore, the number of transmission channels and their transmission probabilities could be determined by the simultaneous conductance and shot noise measurements. The simultaneous shot noise and conductance measurements have been performed for single $H_2$, benzene, and water molecular junctions.[17,99–101] Fig. 21 shows the shot noise for the single $D_2$–Pt molecular junctions as a function of bias current.[99] The transmission probabilities were ($\tau_1$ = 0.995, $\tau_2$ = 0.015) for the $D_2$–Pt junctions with zero bias conductance of 1.01 $G_0$. The number of channels was close to one, indicating that the number of the molecules bridging Pt electrodes was one.

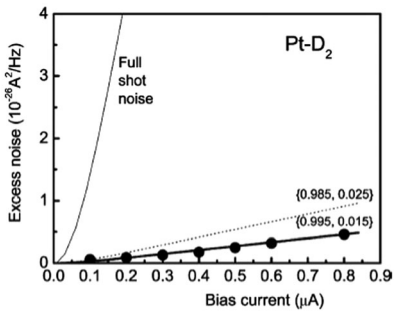


**Fig. 21** Shot noise as a function of the bias current across the $D_2$–Pt junction. Fitting the data with theory (curves) gives the decomposition of the total transmission in terms of transmission probabilities, $\tau_i$, of the conduction channels as shown in the inset.[99]

## Single molecular devices

Finally, we briefly comment on the experimental challenges to developing single molecular devices. A single molecular transistor was reported for single BDT and alkanedithiol molecular junctions. Song *et al.* prepared a very thin gate oxide layer (3 nm thick $Al_2O_3$) by natural oxidation of Al. Electron current could be directly modulated by an external gate voltage. The direct molecular orbital gating was clearly shown by the TVS.[18]

A single molecular diode was reported for non-symmetric diblock dipyrimidinyldiphenyl molecules using the STM-BJ technique. The orientation of the non-symmetric molecule was controlled through a selective deprotection strategy. The non-symmetric molecule was terminated with two different protecting groups, trimethylsilylethyl (dipyrimidinyl side) and cyanoethyl (diphenyl side). The first deprotection step removed the cyanoethyl protecting group, which allowed a SAM to form on the gold substrate of the diblock non-symmetric molecules with the diphenyl end bound to the substrate. The second step removed the trimethylsilylethyl group, which exposes the thiol group at the dipyrimidinyl end to the tip electrode. The resulting single non-symmetric molecular junction exhibited pronounced rectification behavior, with current flowing from the dipyrimidinyl to the diphenyl moieties.[19]

Single molecular switches were reported for a photochromic molecule and for *E*–*Z* isomers.[102,103] Fig. 22 shows the schematic view of the single molecular junction of the photochromic molecule.[102] The resistance of the single molecular junction after switching was about three orders of magnitude larger than that of the initial value. Recently, mechanical configuration switches have attracted wide attention, because the operation mechanism is characteristic of the single molecular junction, in contrast to the above-mentioned single molecular devices. The conductance of a single molecular junction depends on the strength of the molecule–metal coupling ($\Gamma$). When the

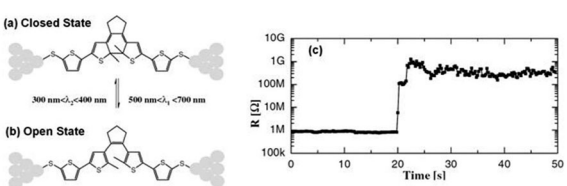


**Fig. 22** Photochromic molecular switch between two Au contacts in closed state (a) and open state. (b) Resistance *vs.* time. At $t$ = 0, a lamp is turned on. After approximately 20 s, a clear jump is observed (1 V bias).[102]

strength of the molecule–metal coupling can be modulated by mechanical control, the conductance of the single molecular junction could be controlled. The mechanically controlled binary conductance switching has been reported for bipyridine, alkanedithiol, and oligoene.[20,104]

## Conclusions

In this review, we discussed the fabrication, electron transport mechanisms, and characterization of single molecular junctions. The recent development of fabrication techniques such as STM-BJ and MCBJ enables us to investigate the electron transport properties of a variety of molecules. A series of investigations on the single molecular junction reveal that the conductance of the single molecular junction depends on the strength of the metal–molecule coupling, the energy difference between the conduction orbital and the Fermi level of the metal electrodes, and the degree of π-conjugation. The conductance of the single molecular junction can be controlled by tuning these factors. We also discuss the basic research relating to hopping and tunneling electron transport, and electron transport through the π-stacked system. The characterization of the single molecular junction becomes important, in order to fully understand and control its properties. IETS, PCS, and SERS have been applied to single molecular junction in order to characterize its atomic configuration. Thermopower, shot noise, and transition voltage spectroscopy have been investigated in order to characterize the electronic structure of the single molecular junction.

The interaction between the conduction electron and its spin is becoming a hot topic, due to its potential application in molecular spintronics, although we did not comment on this topic.[105–107] The Kondo peak is observed in the *I–V* curve of a single molecular junction, when the localized spin interacts with the conduction electron. The Kondo effect has been observed for a single Co complex molecular junction.[106] Recently, the splitting of the Kondo peak induced by mechanical stretching was reported for a single Co complex molecular junction. The splitting of the Kondo peak is explained by the change in the spin states by mechanical stretching.[107]

Developing the novel properties of the single molecular junction and controlling them will be central topics in this research field in the coming years. In most of the investigations on single molecular junctions, their properties are discussed based on the characteristics of the isolated molecule. For example, a single molecular photo switch has been investigated using photochromic molecules. However, the performance of a single molecular photo switch is much lower than that of the bulk. The single molecular junction using photochromic molecules did not switch from the off state to the on state, though it switched from the on state to the off state *via* photo radiation. It is important to find novel functions that are unique characteristics of the single molecular junction. One of the possibilities is chemical reactions at the single molecular junction, which proceed at the metal–molecule interface. In the single molecular junction, the molecule interacts with the metal surface *via* two interfaces. We can expect novel chemical reactions at this junction.

In this review, we do not mention the current topics in the theoretical calculation of the single molecule junction. The first-principles calculations using non-equilibrium Green's function theory (NEGF) combined with DFT can reveal the electron transport mechanism and electronic structures of the single molecule junction. The molecular dynamic simulation can reveal the formation and breaking process of the molecular junction. The disagreement between theoretical calculation and experimental results was large, due to the underestimation of the HOMO–LUMO gap. The recent development of theoretical calculation is overcoming these problems.[1–9]

## Acknowledgements

We have profited from many discussions with Prof. K. Murakoshi, Prof. J. M. van Ruitenbeeek, Prof. M. Fujita, Mr Y. Takahashi, and Miss T. Nakazumi. This work was financially supported by Grants-in-Aids for Scientific Research on Priority Areas (No. 17069001), Scientific Research in Innovative Areas (No. 23111706) and Grant-in-Aid for Scientific Research (A) and (B) (No. 21340074 and No. 24245027) from the Ministry of Education, Culture, Sports, Science and Technology (MEXT) and Sumitomo, Iketani, Murata, Kao, and Asahi Glass foundation. S.K. was supported by Grant-in-Aid for JSPS Research Fellow.

## References

1 J. C. Cuevas and E. Scheer, *Molecular Electronics: An Introduction to Theory and Experiment*, World Scientific Publishing Co. Pte. Ltd., Singapore, 2010.
2 N. Agraït, A. L. Yeyati and J. M. van Ruitenbeek, *Phys. Rep.*, 2003, **377**, 81–279.
3 *Introducing Molecular Electronics*, ed. G. Cuniberti, G. Fagas and K. Richter, Springer-Verlag, Berlin, Heidelberg, 2005.
4 N. J. Tao, *Nat. Nanotechnol.*, 2006, **1**, 173.
5 M. Kiguchi and S. Kaneko, *ChemPhysChem*, 2012, **13**, 1116–1126.
6 H. B. Akkerman and B. de Boer, *J. Phys.: Condens. Matter*, 2008, **20**, 013001.
7 R. L. McCreery and A. J. Bergren, *Adv. Mater.*, 2009, **21**, 4303.
8 B. Ulgut and H. D. Abruna, *Chem. Rev.*, 2008, **108**, 2721.
9 H. Song, M. A. Reed and T. Lee, *Adv. Mater.*, 2011, **23**, 1583–1608.
10 A. Aviram and M. A. Ratner, *Chem. Phys. Lett.*, 1974, **29**, 277–283.
11 M. A. Reed, C. Zhou, C. J. Muller, T. P. Burgin and J. M. Tour, *Science*, 1997, **278**, 252–254.
12 X. D. Cui, A. Primak, X. Zarate, J. Tomfohr, O. F. Sankey, A. L. Moore, T. A. Moore, D. Gust, G. Harris and S. M. Lindsay, *Science*, 2001, **294**, 571–574.
13 B. Xu and N. J. Tao, *Science*, 2003, **301**, 1221–1223.

 

14 L. Venkataraman, J. E. Klare, C. Nuckolls, M. S. Hybertsen and M. L. Steigerwald, *Nature*, 2006, **442**, 904–907.
15 G. Sedghi, V. M. García-Suárez, L. J. Esdaile, H. L. Anderson, C. J. Lambert, S. Martín, D. Bethell, S. J. Higgins, M. Elliott, N. Bennett, J. E. Macdonald and R. J. Nichols, *Nat. Nanotechnol.*, 2011, **6**, 517–523.
16 M. Kiguchi, T. Takahashi, Y. Takahashi, Y. Yamauchi, T. Murase, M. Fujita, T. Tada and S. Watanabe, *Angew. Chem., Int. Ed.*, 2011, **50**, 5708–5711.
17 M. Kiguchi, O. Tal, S. Wohlthat, F. Pauly, M. Krieger, D. Djukic, J. C. Cuevas and J. M. van Ruitenbeek, *Phys. Rev. Lett.*, 2008, **101**, 046801.
18 H. Song, Y. Kim, Y. H. Jang, H. Jeong, M. A. Reed and T. Lee, *Nature*, 2009, **462**, 1039–1043.
19 I. Dez-Perez, J. Hihath, Y. Lee, L. Yu, L. Adamska, M. A. Kozhushner, I. I. Oleynik and N. Tao, *Nat. Chem.*, 2009, **1**, 635–641.
20 O. Tal, M. Krieger, B. Leerink and J. M. van Ruitenbeek, *Phys. Rev. Lett.*, 2008, **100**, 196804.
21 P. Reddy, S. Jang, R. A. Segalman and A. Majumdar, *Science*, 2007, **315**, 1568–1571.
22 (*a*) R. H. M. Smit, Y. Noat, C. Untiedt, N. D. Lang, M. C. van Hemert and J. M. van Ruitenbeek, *Nature*, 2002, **419**, 906–909; (*b*) D. Djukic, K. S. Thygesen, C. Untiedt, R. H. M. Smit, K. W. Jacobsen and J. M. van Ruitenbeek, *Phys. Rev. B: Condens. Matter Mater. Phys.*, 2005, **71**, 161402.
23 Z. Liu, S. Ding, Z. Chen, X. Wang, J. Tian, J. R. Anema, X. Zhou, D. Wu, B. Mao, X. Xu, B. Ren and Z. Tian, *Nat. Commun.*, 2011, **2**, 1310.
24 W. Wang, T. Lee, I. Kretzschmar and M. A. Reed, *Nano Lett.*, 2004, **4**, 643–646.
25 N. Tuccitto, V. Ferri, M. Cavazzini, S. Quici, G. Zhavnerko, A. Licciardello and M. A. Rampi, *Nat. Mater.*, 2009, **8**, 41–46.
26 S. H. Choi, B. S. Kim and C. D. Frisbie, *Science*, 2008, **320**, 1482–1485.
27 T. Dadosh, Y. Gordin, R. Krahne, I. Khivrich, D. Mahalu, V. Frydman, J. Sperling, A. Yacoby and I. Bar-Joseph, *Nature*, 2005, **436**, 677–680.
28 (*a*) L. Venkataraman, Y. S. Park, A. C. Whalley, C. Nuckolls, M. S. Hybertsen and M. L. Steigerwald, *Nano Lett.*, 2007, **7**, 502–506; (*b*) M. Kiguchi, S. Miura, K. Hara, M. Sawamura and K. Murakochi, *Appl. Phys. Lett.*, 2006, **89**, 213104.
29 X. Xiao, B. Xu and N. J. Tao, *Nano Lett.*, 2004, **4**, 267–271.
30 W. Haiss, H. van Zalinge, S. J. Higgins, D. Bethell, H. Hobenreich, D. J. Schiffrin and R. J. Nichols, *J. Am. Chem. Soc.*, 2003, **125**, 15294–15295.
31 W. Haiss, R. J. Nichols, H. van Zalinge, S. J. Higgins, D. Bethell and D. J. Schiffrin, *Phys. Chem. Chem. Phys.*, 2004, **6**, 4330–4337.
32 W. Haiss, C. Wang, I. Grace, A. Batsanov, D. J. Schiffrin, S. J. Higgins, M. R. Bryce, C. J. Lambert and R. J. Nichols, *Nat. Mater.*, 2006, **5**, 995–1002.
33 J. M. van Ruitenbeek, A. Alvarez, I. Piñeyro, C. Grahmann, P. Joyez, M. H. Devoret, D. Esteve and C. Urbina, *Rev. Sci. Instrum.*, 1996, **67**, 108–111.
34 (*a*) T. Nakazumi, Y. Wada and M. Kiguchi, *Nanotechnology*, 2012, **23**, 405702; (*b*) M. Kiguchi, D. Djukic and J. M. van Ruitenbeek, *Nanotechnology*, 2007, **18**, 035205; (*c*) M. Tsutsui, K. Shoji, M. Taniguchi and T. Kawai, *Nano Lett.*, 2008, **8**, 345–349.
35 D. Dulić, F. Pump, S. Campidelli, P. Lavie, G. Cuniberti and A. Filoramo, *Angew. Chem., Int. Ed.*, 2009, **48**, 8273–8276.
36 R. S. Klausen, J. R. Widawsky, M. L. Steigerwald, L. Venkataraman and C. Nuckolls, *J. Am. Chem. Soc.*, 2012, **134**, 4541–4544.
37 M. Kiguchi, S. Miura, T. Takahashi, K. Hara, M. Sawamura and K. Murakoshi, *J. Phys. Chem. C*, 2008, **112**, 13349–13352.
38 F. Chen, X. Li, J. Hihath, Z. Huang and N. J. Tao, *J. Am. Chem. Soc.*, 2006, **128**, 15874–15881.
39 W. Hong, D. Z. Manrique, P. Moreno-Garcia, M. Gulcur, A. Mishchenko, C. J. Lambert, M. R. Bryce and T. Wandlowski, *J. Am. Chem. Soc.*, 2012, **134**, 2292–2304.
40 L. Venkataraman, J. E. Klare, I. W. Tam, C. Nuckolls, M. S. Hybertsen and M. Steigerwald, *Nano Lett.*, 2006, **6**, 458–462.
41 A. Mishchenko, L. A. Zotti, D. Vonlanthen, M. Bürkle, F. Pauly, J. C. Cuevas, M. Mayor and T. Wandlowski, *J. Am. Chem. Soc.*, 2011, **133**, 184–187.
42 L. Venkataraman, Y. S. Park, A. C. Whalley, C. Nuckolls, M. S. Hybertsen and M. L. Steigerwald, *Nano Lett.*, 2007, **7**, 502–506.
43 R. Parameswaran, J. R. Widawsky, H. Vázquez, Y. S. Park, B. M. Boardman, C. Nuckolls, M. L. Steigerwald, M. S. Hybertsen and L. Venkataraman, *J. Phys. Chem. Lett.*, 2010, **1**, 2114–2119.
44 Y. S. Park, A. C. Whalley, M. Kamenetska, M. L. Steigerwald, M. S. Hybertsen, C. Nuckolls and L. Venkataraman, *J. Am. Chem. Soc.*, 2007, **129**, 15768–15769.
45 K. Yokota, M. Taniguchi, H. Tanaka and T. Kawai, *Phys. Rev. B: Condens. Matter Mater. Phys.*, 2008, **77**, 165416.
46 A. Fukazawa, M. Kiguchi, S. Tange, Y. Ichihashi, Q. Zhao, T. Takahashi, T. Konishi, K. Murakoshi, Y. Tsuji, A. Staykov, K. Yoshizawa and S. Yamaguchi, *Chem. Lett.*, 2011, **40**, 174–176.
47 J. M. Seminario, C. E. De La Cruz and P.A. Derosa, *J. Am. Chem. Soc.*, 2001, **123**, 5616–5617.
48 Z. Li and D. S. Kosov, *Phys. Rev. B: Condens. Matter Mater. Phys.*, 2007, **76**, 035415.
49 M. Kiguchi, T. Takahashi, M. Kanehara, T. Teranishi and K. Murakoshi, *J. Phys. Chem. C*, 2009, **113**, 9014–9017.
50 M. L. Perrin, F. Prins, C. A. Martin, A. J. Shaikh, R. Eelkema, Jan H. van Esch, T. Briza, R. Kaplanek, V. Kral, J. M. van Ruitenbeek, H. S. J. van der Zant and D. Dulić, *Angew. Chem., Int. Ed.*, 2011, **50**, 11223–11226.
51 C. A. Martin, D. Ding, J. K. Sørensen, T. Bjørnholm, J. M. van Ruitenbeek and H. S. J. van der Zant, *J. Am. Chem. Soc.*, 2008, **130**, 13198–13199.
52 M. Kiguchi, S. Miura, K. Hara, M. Sawamura and K. Murakoshi, *Appl. Phys. Lett.*, 2007, **91**, 053110.
53 C.-H. Ko, M.-J. Huang, M.-D. Fu and C.-H. Chen, *J. Am. Chem. Soc.*, 2010, **132**, 756–764.

54 Y. Ie, T. Hirose, H. Nakamura, M. Kiguchi, N. Takagi, M. Kawai and Yoshio Aso, *J. Am. Chem. Soc.*, 2011, **133**, 3014–3022.
55 Z. Li and E. Borguet, *J. Am. Chem. Soc.*, 2011, **134**, 63–66.
56 M. Kiguchi, K. Tahara, Y. Takahashi, K. Hasui and Y. Tobe, *Chem. Lett.*, 2010, 788–789.
57 D. M. Cardamone, C. A. Stafford and S. Mazumdar, *Nano Lett.*, 2006, **6**, 2422–2426.
58 K. Tagami, L. Wang and M. Tsukada, *Nano Lett.*, 2004, **4**, 209–212.
59 T. Hansen, G. C. Solomon, D. Q. Andrews and M. A. Ratner, *J. Chem. Phys.*, 2009, **131**, 194704.
60 S. H. Ke, W. Yang and H. U. Baranger, *Nano Lett.*, 2008, **8**, 3257–3262.
61 M. Kiguchi, H. Nakamura, Y. Takahashi, T. Takahashi and T. Ohto, *J. Phys. Chem. C*, 2010, **114**, 22254–22261.
62 C. M. Guédon, H. Valkenier, T. Markussen, K. S. Thygesen, J. C. Hummelen and S. J. van der Molen, *Nat. Nanotechnol.*, 2012, **7**, 305–309.
63 (*a*) S. Kaneko, T. Nakazumi and M. Kiguchi, *J. Phys. Chem. Lett.*, 2010, **1**, 3520–3523; (*b*) M. Kiguchi, *Appl. Phys. Lett.*, 2009, **95**, 073301; (*c*) S. Kaneko, L. Wang, G. Luo, J. Lu, S. Nagase, S. Sato, M. Yamada, Z. Slanina, T. Akasaka and M. Kiguchi, *Phys. Rev. B: Condens. Matter Mater. Phys.*, 2012, **86**, 155406.
64 M. Kiguchi and K. Murakoshi, *J. Phys. Chem. C*, 2008, **112**, 8140–8143.
65 (*a*) T. Nakazumi, S. Kaneko, R. Matsushita and M. Kiguchi, *J. Phys. Chem. C*, 2012, **116**, 18250–18255; (*b*) Y. Guo, M. Kiguchi, J. Zhao and K. Murakoshi, *Chem. Phys. Lett.*, 2009, **477**, 189–193; (*c*) O. Tal, M. Kiguchi, W. H. A. Thijssen, D. Djukic, C. Untiedt, R. H. M. Smit and J. M. van Ruitenbeek, *Phys. Rev. B: Condens. Matter Mater. Phys.*, 2009, **80**, 085427.
66 M. Taniguchi, M. Tsutsui, K. Shoji, H. Fujiwara and T. Kawai, *J. Am. Chem. Soc.*, 2009, **131**, 14146–14147.
67 I. Diez-Perez, J. Hihath, T. Hines, Z. Wang, G. Zhou, K. Mullen and N. Tao, *Nat. Nanotechnol.*, 2011, **6**, 226–231.
68 S. Y. Quek, M. Kamenetska, M. L. Steigerwald, H. J. Choi, S. G. Louie, M. S. Hybertsen, J. B. Neaton and L. Venkataraman, *Nat. Nanotechnol.*, 2009, **4**, 230–234.
69 Z. L. Cheng, R. Skouta, H. Vazquez, J. R. Widawsky, S. Schneebeli, W. Chen, M. S. Hybertsen, R. Breslow and L. Venkataraman, *Nat. Nanotechnol.*, 2011, **6**, 353–357.
70 G. Sedghi, K. Sawada, L. J. Esdaile, M. Hoffmann, H. L. Anderson, D. Bethell, W. Haiss, S. J. Higgins and R. J. Nichols, *J. Am. Chem. Soc.*, 2008, **130**, 8582–8583.
71 R. Yamada, H. Kumazawa, S. Tanaka and H. Tada, *Appl. Phys. Express*, 2009, **2**, 025002.
72 S. Woitellier, J. P. Launay and C. Joachim, *Chem. Phys.*, 1989, **131**, 481–488.
73 M. Dell'Angela, G. Kladnik, A. Cossaro, A. Verdini, M. Kamenetska, I. Tamblyn, S. Y. Quek, J. B. Neaton, D. Cvetko, A. Morgante and L. Venkataraman, *Nano Lett.*, 2010, **10**, 2470–2474.
74 B. Xu, X. Xiao, X. Yang, L. Zang and N. J. Tao, *J. Am. Chem. Soc.*, 2005, **127**, 2386–2387.
75 X. Li, J. Hihath, F. Chen, T. Masuda, L. Zang and N. J Tao, *J. Am. Chem. Soc.*, 2007, **129**, 11535–11542.
76 A. Tawara, T. Tada and S. Watanabe, *Phys. Rev. B: Condens. Matter Mater. Phys.*, 2006, **80**, 073409.
77 V. Fatemi, M. Kamenetska, J. B. Neaton and L. Venkataraman, *Nano Lett.*, 2011, **11**, 1988–1992.
78 S. Nakashima, Y. Takahashi and M. Kiguchi, *Beilstein J. Nanotechnol.*, 2011, **2**, 755–759.
79 E. Leary, H. Hobenreich, S. J. Higgins, H. van Zalinge, W. Haiss, R. J. Nichols, C. M. Finch, I. Grace, C. J. Lambert, R. McGrath and J. Smerdon, *Phys. Rev. Lett.*, 2009, **102**, 086801.
80 J. C. Genereux and J. K. Barton, *Chem. Rev.*, 2010, **110**, 1642–1662; J. Wu, W. Pisula and K. Mullen, *Chem. Rev.*, 2007, **107**, 718–747; M. Bendikov, F. Wudl and D. F. Perepichka, *Chem. Rev.*, 2004, **104**, 4891–4945.
81 S. T. Schneebeli, M. Kamenetska, Z. Cheng, R. Skouta, R. A. Friesner, L. Venkataraman and R. Breslow, *J. Am. Chem. Soc.*, 2011, **133**, 2136–2139.
82 S. Wu, M. T. González, R. Huber, S. Grunder, M. Mayor, C. Schönenberger and M. Calame, *Nat. Nanotechnol.*, 2008, **3**, 569–574.
83 S. Martin, I. Grace, M. R. Bryce, C. Wang, R. Jitchati, A. S. Batsanov, S. J. Higgins, C. J. Lambert and R. J. Nichols, *J. Am. Chem. Soc.*, 2010, **132**, 9157–9164.
84 R. B. Pontes, F. D. Novaes, A. Fazzio and A. J. R. da Silva, *J. Am. Chem. Soc.*, 2006, **128**, 8996–8997.
85 G. C. Solomon, C. Herrmann, J. Vura-Weis, M. R. Wasielewski and M. A. Ratner, *J. Am. Chem. Soc.*, 2010, **132**, 7887–7889.
86 J. Hihath, C. R. Arroyo, G. Rubio-Bollinger, N. Tao and N. Agraït, *Nano Lett.*, 2008, **8**, 1673–1678.
87 M. Kiguchi, T. Nakazumi, K. Hashimoto and K. Murakoshi, *Phys. Rev. B: Condens. Matter Mater. Phys.*, 2010, **81**, 045420.
88 R. Matsushita, S. Kaneko, T. Nakazumi and M. Kiguchi, *Phys. Rev. B: Condens. Matter Mater. Phys.*, 2011, **84**, 245412.
89 M. Paulsson, T. Frederiksen, H. Ueba, N. Lorente and M. Brandbyge, *Phys. Rev. Lett.*, 2008, **100**, 226604.
90 Y. Kim, T. Pietsch, A. Erbe, W. Belzig and E. Scheer, *Nano Lett.*, 2011, **11**, 3734–3738.
91 (*a*) D. R. Ward, N. J. Halas, J. W. Ciszek, J. M. Tour, Y. Wu, P. Nordlander and D. Natelson, *Nano Lett.*, 2008, **8**, 919–924; (*b*) T. Konishi, M. Kiguchi, M. Takase, F. Nagasawa, H. Nabika, K. Ikeda, K. Uosaki, K. Ueno, H. Misawa and K. Murakoshi, *J. Am. Chem. Soc.*, DOI: 10.1021/ja307821u.
92 J. Tian, B. Liu, X. Li, Z. Yang, B. Ren, S. Wu, N. Tao and Z. Tian, *J. Am. Chem. Soc.*, 2006, **128**, 14748–14749.
93 E. H. Huisman, C. M. Guédon, B. J. van Wees and S. Jan van der Molen, *Nano Lett.*, 2009, **9**, 3909–3913.
94 M. Araidai and M. Tsukada, *Phys. Rev. B: Condens. Matter Mater. Phys.*, 2010, **81**, 235114.
95 (*a*) S. Guo, J. Hihath, I. Díez-Perez and N. Tao, *J. Am. Chem. Soc.*, 2011, **133**, 19189–19197; (*b*) I. Bâldea, *J. Am. Chem. Soc.*, 2012, **134**, 7958–7962.
96 A. Tan, J. Balachandran, S. Sadat, V. Gavini, B. D. Dunietz, S. Jang and P. Reddy, *J. Am. Chem. Soc.*, 2011, **133**, 8838–8841.
97 S. K. Yee, J. A. Malen, A. Majumdar and R. A. Segalman, *Nano Lett.*, 2011, **11**, 4089–4094.

 

98 B. Xu, X. Xiao and N. J. Tao, *J. Am. Chem. Soc.*, 2003, **125**, 16164–16165.
99 D. Djukic and J. M. van Ruitenbeek, *Nano Lett.*, 2006, **6**, 789–793.
100 M. Kiguchi, R. Stadler, I. S. Kristensen, D. Djukic and J. M. van Ruitenbeek, *Phys. Rev. Lett.*, 2007, **98**, 146802.
101 O. Tal, M. Krieger, B. Leerink and J. M. van Ruitenbeek, *Phys. Rev. Lett.*, 2008, **100**, 196804.
102 D. Dulic, S. J. van der Molen, T. Kudernac, H. T. Jonkman, J. J. D. de Jong, T. N. Bowden, J. van Esch, B. L. Feringa and B. J. van Wees, *Phys. Rev. Lett.*, 2003, **91**, 207402.
103 S. Martin, W. Haiss, S. J. Higgins and R. J. Nichols, *Nano Lett.*, 2010, **10**, 2019–2023.
104 J. S. Meisner, M. Kamenetska, M. Krikorian, M. L. Steigerwald, L. Venkataraman and C. Nuckolls, *Nano Lett.*, 2011, **11**, 1575–1579.
105 M. Ternes, A. J Heinrich and W. Schneider, *J. Phys.: Condens. Matter*, 2009, **21**, 053001.
106 J. Park, A. N. Pasupathy, J. I. Goldsmith, C. Chang, Y. Yaish, J. R. Petta, M. Rinkoski, J. P. Sethna, H. D. Abruña, P. L. McEuen and D. C. Ralph, *Nature*, 2002, **417**, 722–725.
107 J. J. Parks, A. R. Champagne, T. A. Costi, W. W. Shum, A. N. Pasupathy, E. Neuscamman, S. Flores-Torres, P. S. Cornaglia, A. A. Aligia, C. A. Balseiro, G. K.-L. Chan, H. D. Abruña and D. C. Ralph, *Science*, 2010, **328**, 1370–1373.